View metadata, citation and similar papers at core.ac.uk
brought to you by CORE
provided by Defence Science Journal

Defence Science Journal, Vol 50, No 2, April 2000, pp. 37-146
© 2000, DESIDOC

Velocity Distribution in the Annuli of a Plane Reverse-Flow Combustor Model

Sanjeev Bharani, S.N. Singh and D.P. Agrawal
Indian Institute of Technology, New Delhi – 110 016

ABSTRACT

This paper reports the velocity profiles and flow distribution in the annuli of a plane reverse-flow gas turbine combustor model. Based on these, flow-split through different liner holes and swirlers has been estimated. It is seen that percentage flow-split through the outer liner surface holes, compared to that through liner dome and inner liner surface holes, is not affected significantly by increase in the inlet flow velocity.

NOMENCLATURE

Re	Reynolds number
t	Annular passage height at the plane of measurement
Ux	Axial velocity
Uavi	Mean inlet velocity
Uy	Transverse velocity
z	Measurement location from the liner surface
ν	Kinematic viscosity

1. INTRODUCTION

Annular reverse-flow combustors are widely used[1] in small gas turbine engines. Simple methodology of sub-component investigation to map and analyse flow in gas turbine combustors has been in practice due to their complex geometry. Various investigations pertaining to straight-through combustors are available in literature[2-8], but the reported studies on reverse-flow combustors are limited. The results of straight-through combustors also do not correlate fully with the reverse-flow designs due to basic difference in the two geometries.

Studies reported on reverse-flow combustors pertain to the behaviour of primary and dilution jets in the combustor liner and the turn section[9-14]. Flow characteristics in a liner are dependent on the flow characteristics in the surrounding annuli[1]. Literature studies indicate lack of detailed investigations in the annuli of these combustors. Flow characteristics in the outer annulus of a 120 sector model of a reverse-flow combustor along with the flow-splits through the outer liner surface holes have been reported by Bharani[15], *et al.* Flow prediction in the annuli of a reverse-flow combustor has also been attempted by Mohan[16], *et al.* to establish flow-splits through linnmzmnt liner holes. The present study reports an experimental investigation on the flow characteristics in the annuli of a plane reverse-flow combustor model under isothermal conditions. Flow-split through different liner holes has also been evaluated.

Received 22 October 1999

2. COMBUSTOR MODEL

The plane model of a reverse-flow combustor is made up of transparent plexiglass having a span of 300 mm. Figure 1 shows two views of the model along with the locations for measurements at each axial plane, and Table 1 gives its critical geometric details. Air from settling chamber enters the inlet annular passage (12 mm height, plane A), which feeds the outer annulus via a converging passage. The outer annular passage extends around the liner dome and joins the inner annular passage.

The outer and inner liner surfaces have one row each of plunged dilution holes and plain primary holes with a pitch-to-diameter ratio of 4.6 and 9.3, respectively. The dilution holes are in line with the primary holes and are placed just below one another on the two surfaces. The liner dome has two rows of plain cooling holes, one each at the outer and the inner turn, having their axis at 45° wrt to the liner axis. Three swirlers with six curved vanes each are provided in the liner dome head symmetrically placed along the liner mid-plane (x-axis). These swirlers have concentrically fitted fuel pipe. The plane model has most of the complexities of a reverse-flow combustor and still provides easy access to inside passages for measurements. The model has not been provided with the turn section and cooling holes on the liner surfaces. The cooling

Table 1. Geometric details of the plane reverse-flow combustor model

Parameter	Value
Height of the inlet passage (mm)	12.000
Height of the outer annular passage (mm)	
- at plane B	8.500
- at plane C	8.500
- at plane D	7.500
Height of the inner annular passage (mm)	
- at plane E	10.500
- at plane F	11.500
Diameter of the dilution holes (mm)	6.000
Diameter of the primary holes (mm)	3.000
Pitch of the dilution and the primary holes (mm)	28.000
Diameter of the liner dome cooling holes (mm)	1.000
Pitch of the liner dome cooling holes (mm)	4.000
Swirl number	0.875

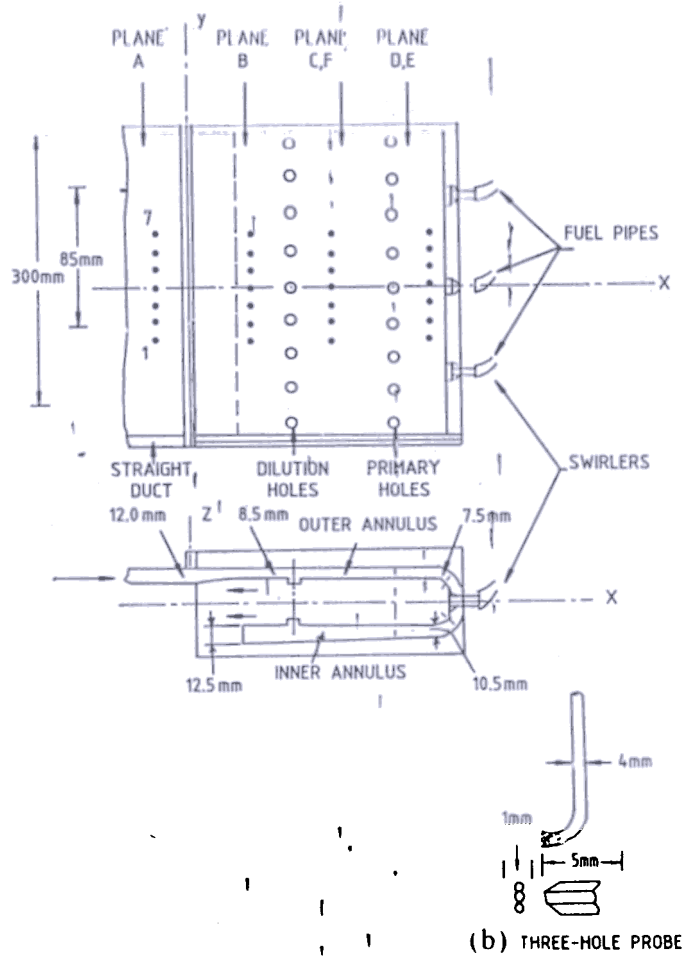

Figure 1. (a) Plane model of reverse-flow combustor and (b) Three-hole probe.

holes on the liner surfaces in prototype are splash cooling holes, which spread the flow parallel to the liner surfaces. The amount of flow-split through these holes is negligible and hence, has not been provided in the plane model. The fuel flow through the fuel pipe has also not been simulated in this study as this does not influence the flow characteristics in the annuli.

3. EXPERIMENTAL SETUP

Figure 2 shows the schematic layout of the experimental setup. Air from the atmosphere was fed to the combustor model by a single-stage centrifugal blower via a rectangular diffuser, a settling chamber and a contraction. To avoid vibrations to be transmitted to the setup, a flexible coupling was used to connect the blower outlet to the diffuser inlet. A 105 mm straight duct was

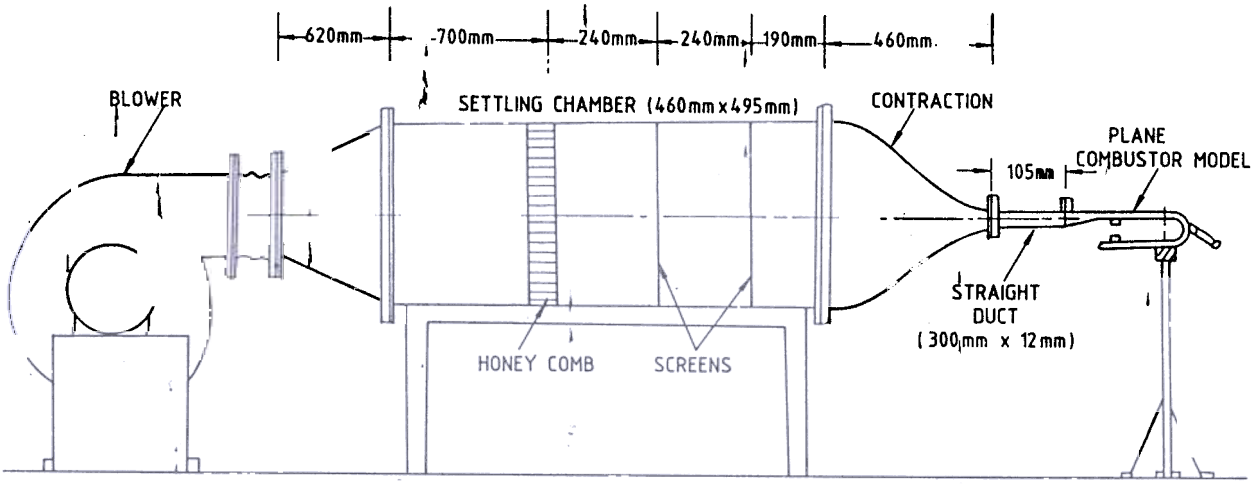

Figure 2. Schematic layout of experimental setup

attached between the exit of the contraction and inlet of the plane model to have settled flow. Measurements of velocity in the annuli were taken at five planes along the axial direction as shown in Fig.1(a) for mean inlet velocities of 11.8 m/s ($Re = 0.95 \times 10^4$) and 17.7 m/s ($Re = 1.42 \times 10^4$) due to limitation of the blower. At each plane, seven measurement locations (only plane A has six) symmetrically placed along the mid-plane (x-axis) were chosen along the transverse direction (y-axis). Measurements were taken with a calibrated miniature three-hole probe using null technique. Figure 1(b) shows the sensing head of the miniature three-hole probe. Three stainless steel tubes (OD = 1.0 mm, ID = 0.5 mm) were with sensing head bent at right angle to the stem. The sensing head of the central tube was perpendicular to its stem axis with two side tubes chamfered at 45° with the central tube axis. Care was taken to clean off burrs from the sensing heads of all the three tubes. The length of the sensing head perpendicular to the main stem was kept small. The maximum blockage based on the dimensions of this probe and flow passage was of the order of 0.14 per cent. Two Debro micromanometers (least count of 0.01 mm) were used to measure the differential pressure sensed by the probe. The estimated uncertainty in the measurements based on the least count of the instruments used is given in Table 2. At each traverse location, both the velocity and the flow angle were measured. Axial and transverse velocities were evaluated using measured the flow angles. These velocity components have been presented in normalised form in Figs 3 to 10.

Table 2. Estimated uncertainty in the experiments

Quantity		Uncertainty
Mean velocity (m/s)	Below 5	± 1.5 %
	Above 5	± 0.5 %
Pressure (m/s)	Below 5	± 2.0 %
	Above 5	± 0.2 %
Angle		± 0.5°

4. RESULTS & DISCUSSION

Results for the lower inlet velocity ($Uavi$ = 11.8 m/s) are presented in Figs 3 to 6, and for the higher inlet velocity ($Uavi$ = 17.7 m/s) in Figs 7 to 10. Figures 3(a) and 3(b) show the axial and transverse velocity profiles obtained at six locations at plane A. They are found akin to an annulus flow with higher velocity near the inner wall, as shown in Fig. 3 (a). Transverse velocity at this plane is nearly zero [Fig. 3 (b)]. The transverse velocities at planes B, C and D were also found close to zero and hence have not been presented.

Figure 4 presents the axial velocity distribution at planes B, C and D. Axial velocities at plane B depict nearly the same nature, as those at inlet plane A, except increase in magnitude due to reduction in the passage height. Axial velocities at plane C [Fig. 4(b)] show two distinct velocity profiles. These profiles at C2, C4 and C6 are highly skewed towards the outer casing wall, whereas at C1, C3, C5 and C7, they are akin to an annulus profile, with

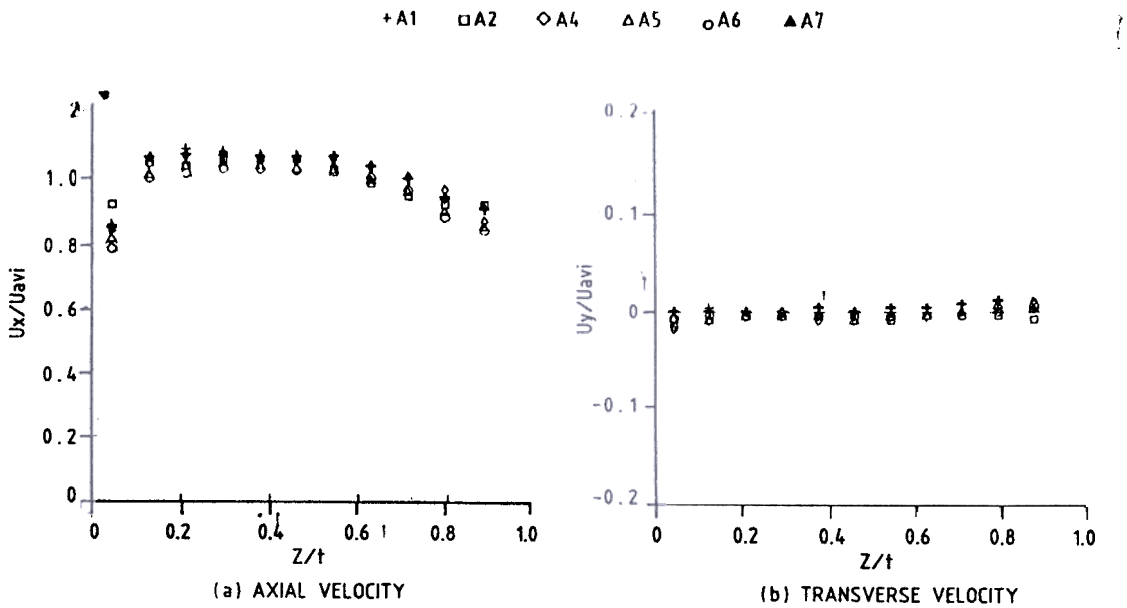

Figure 3. Velocity profiles at inlet plane A (Uavi = 11.80 m/s)

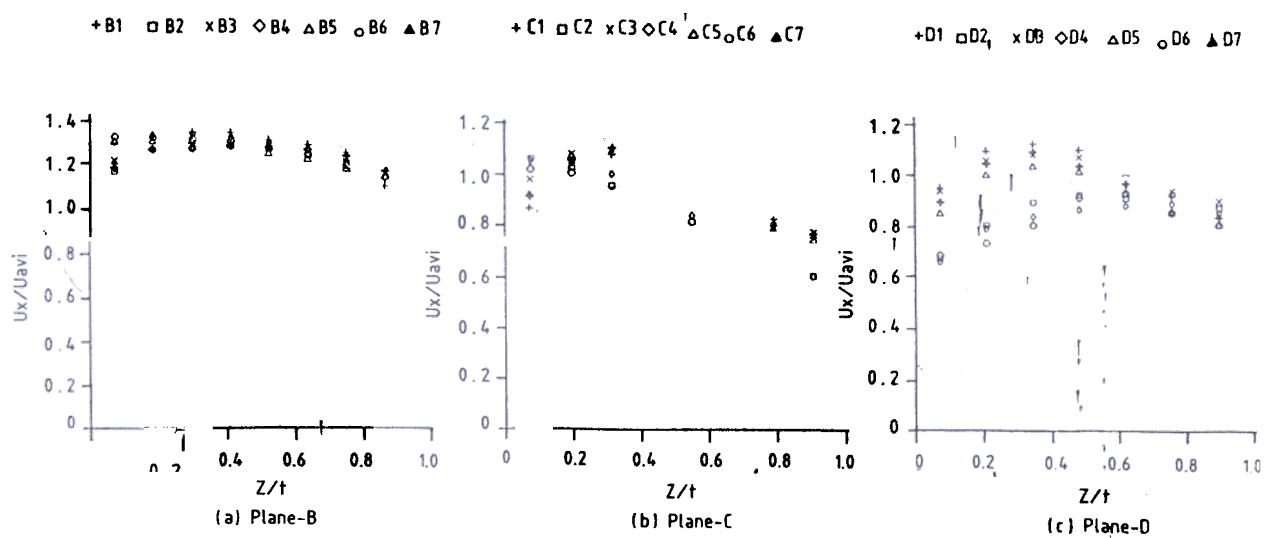

Figure 4. Axial velocity profiles in outer annular passage (Uavi = 11.80 m/s) (a) plane B, (b) plane C, and (c) plane D

lower magnitudes. The skewed nature of profiles can be due to the presence of downstream primary holes for C2, C4 and C6 locations. The fall in velocity magnitude at this plane is due to the large flow-split which occurs at the upstream dilution holes.

Axial velocity profiles at plane D, immediately downstream the outer primary holes, have a nature similar to that of the velocity profiles at plane C, as shown in Fig. 4(c) with further fall in the magnitude due to additional flow-split at the outer primary holes. Figures 5(a) and 5(b) present the velocity profiles in the inner annular passage, just before the row of inner primary holes (plane E), after the flow turns around the liner dome. The flow-split through the swirlers and the cooling holes in the liner dome results in further reduction in axial velocity. The velocity distribution at each measurement location is skewed towards the inner casing wall due to the

bulk flow being deflected outwards with the 180° turn at the liner dome. Measurements were not possible at E3, E4 and E5, close to the liner surface due to wake of the upstream middle swirler body and fuel pipe. Velocity magnitudes at E1 and E7 are the least affected by the wake. The difference in velocity magnitudes at all locations is due to their relative positions vis-a-vis the inner primary holes

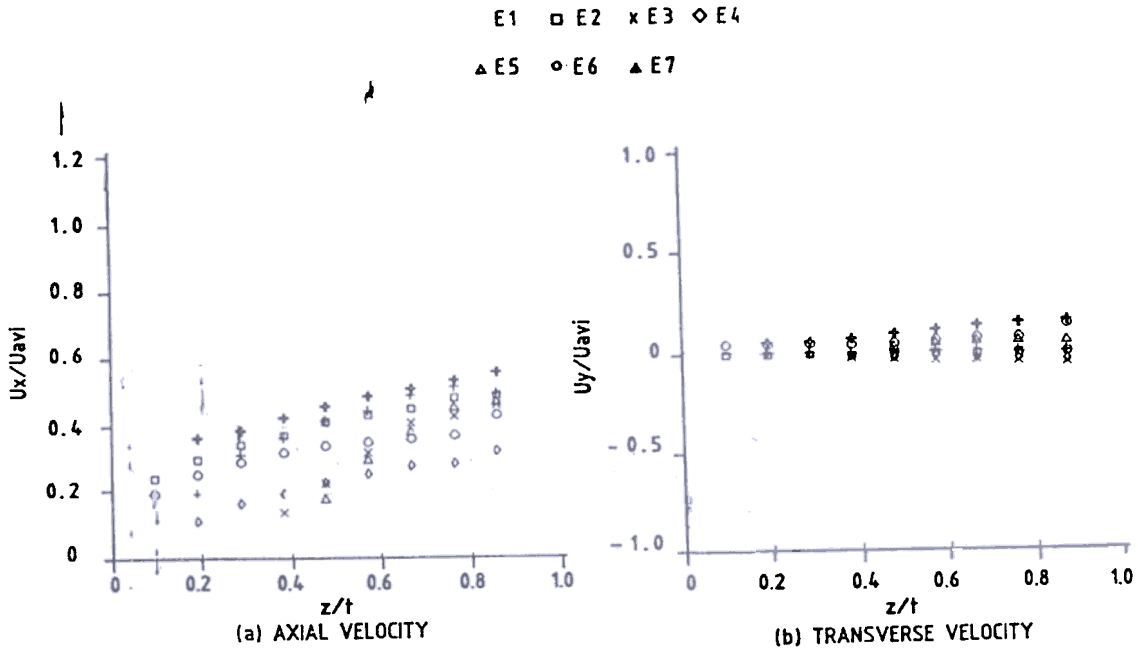

Figure 5. Velocity profiles in inner annular passage, at plane E (Uavi = 11.80 m/s) (a) axial velocity and (b) transverse velocity

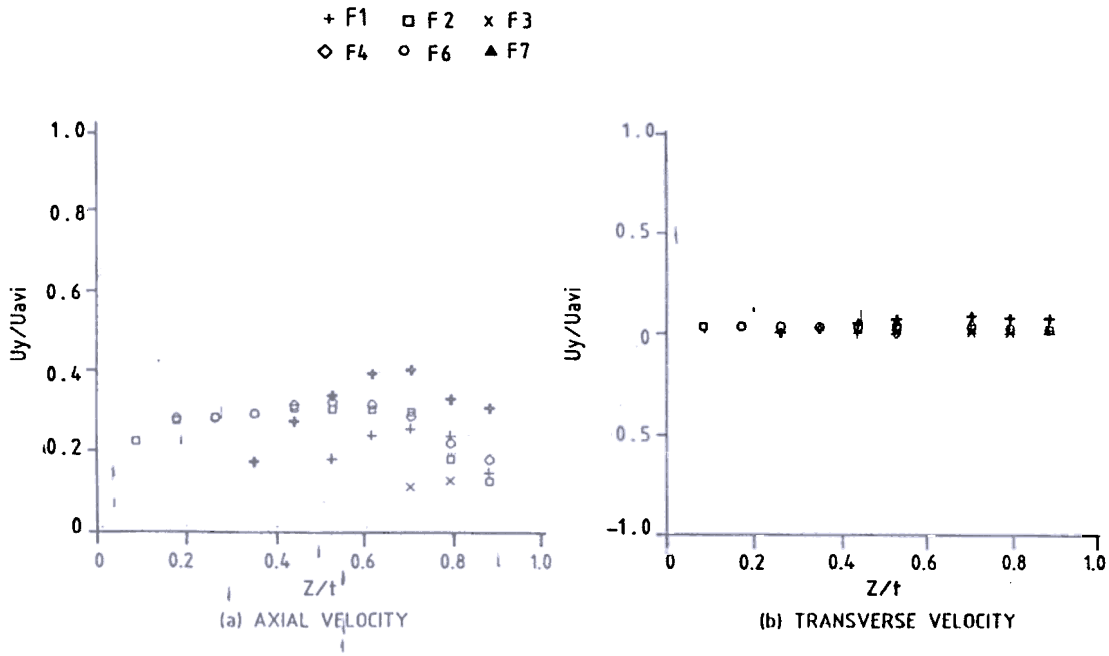

Figure 6. Velocity profiles in inner annular passage, at plane (Uavi = 11.80 m/s) (a) axial velocity and (b) transverse velocity

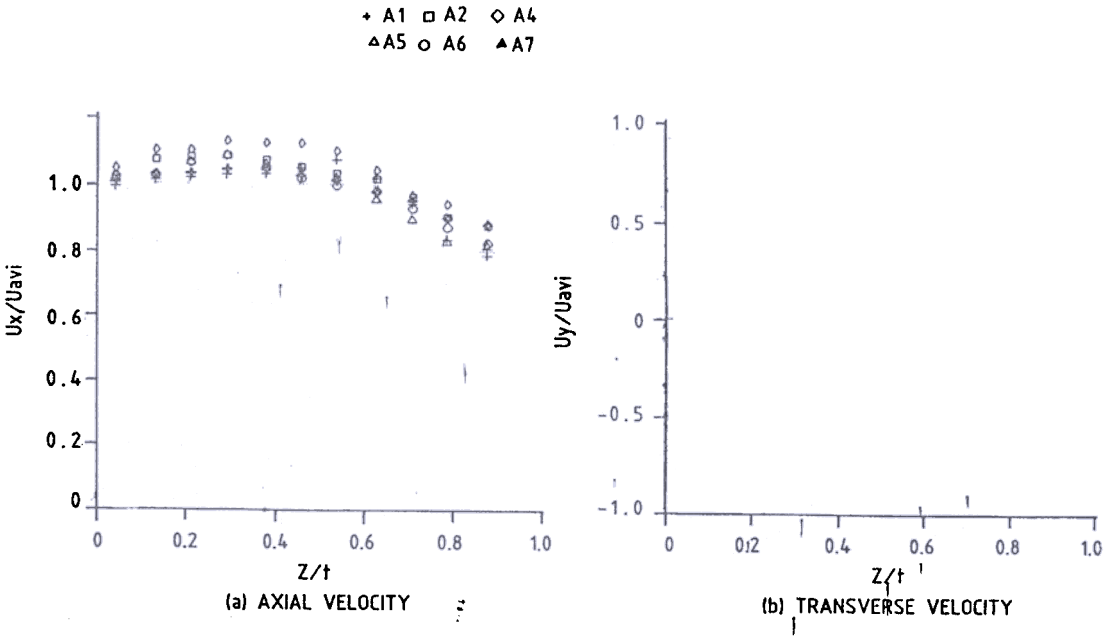

Figure 7. Velocity profiles at inlet plane A (Uavi = 17.70 m/s) (a) axial velocity and (b) transverse velocity

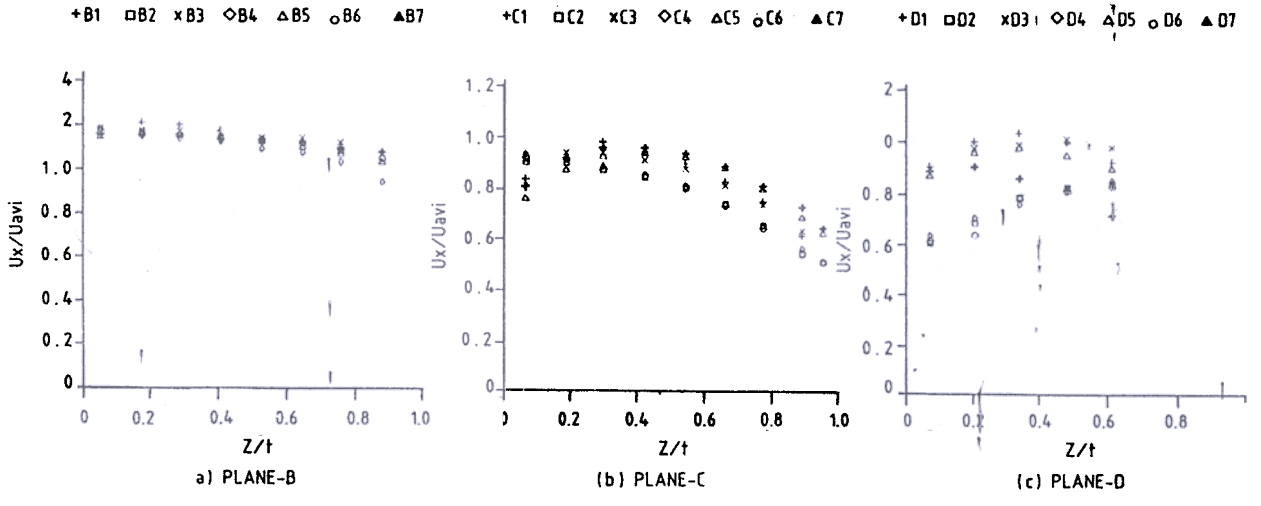

Figure 8. Axial velocity profiles in outer annular passage (Javi = 17.70 m/s) (a) plane B, (b) plane C, and (c) plane D

and the swirler body. Figure 5(b) indicates negligible transverse velocity near the liner wall which increases linearly towards the inner casing wall. This could be due to interference of the bulk flow with the wake of the middle swirler body and fuel pipe.

Velocity profiles at plane F [Figs 6(a) and 6(b)] show that the velocity profiles at locations F1 and F7 are more or less akin to an annulus profile. Velocity profiles are nearly uniform at F2 and F6 locations which are in line with the downstream dilution holes. Measurements at F3, F4 and F5 locations were not possible below *z/t* 0.4. Transverse velocities at this plane are of small magnitudes. The magnitudes near the liner wall are nearly zero and increase slightly towards the inner casing wall.

Measurements at higher inlet velocity show that the velocity profiles in the outer annular passage (plane A, B, C and D) are nearly identical

to the velocity profiles seen at the lower inlet velocity. The major effect of the higher inlet velocity was seen in the inner annular passage. It was observed that the wake due to swirler body and the fuel pipeline vanished and measurements were possible at all the locations of planes E and F. This might be due to higher fluid velocity in the outer annulus which pushed the fluid core to move towards the casing wall as the fluid turned around the upper corner of the liner dome. The flow, while turning around the liner dome, moved along the casing wall and hence filled the inner annular passage fully [Fig.10(a)]. This is also reflected in the flow-split through the liner dome and the inner

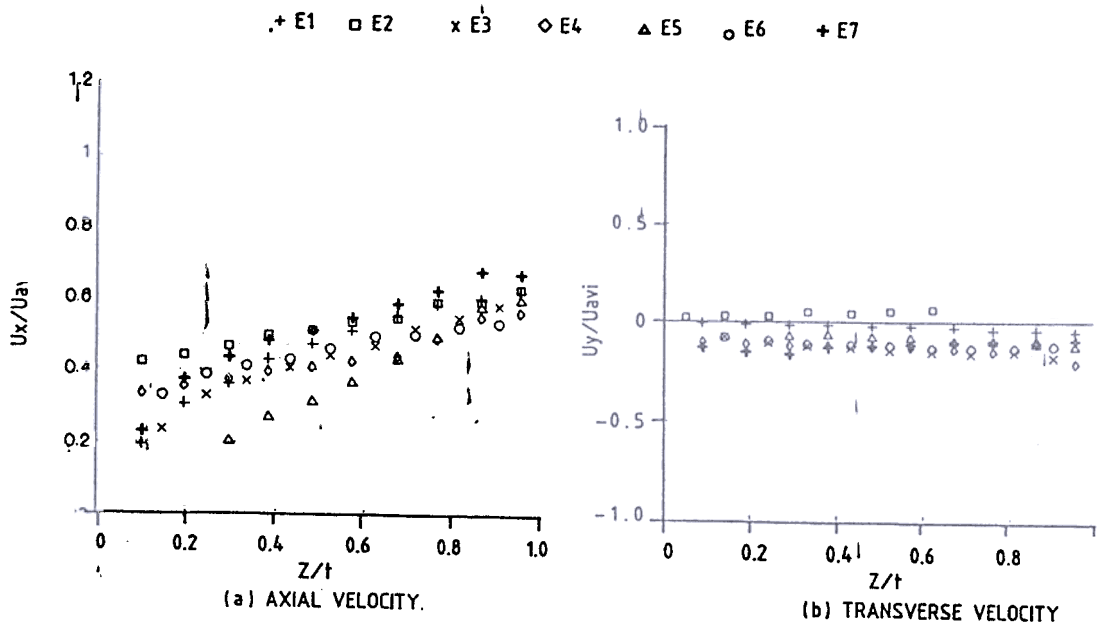

Figure 9. Velocity profiles in inner annular passage, at plane E (Uavi = 17.70 m/s) (a) axial velocity and (b) transverse velocity

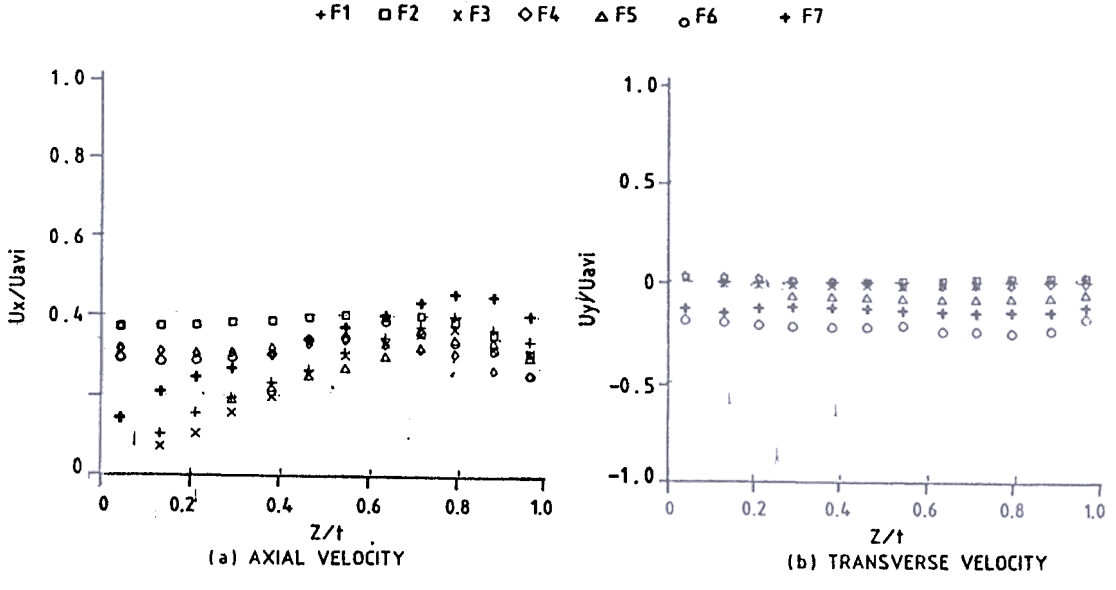

Figure 10. Velocity profiles in inner annular passage, at plane F (Uavi = 17.70 m/s) (a) axial velocity and (b) transverse velocity

annulus. Transverse velocities at this plane [Fig.10(b)] show random behaviour around the zero value, but are nearly uniform across the measurement span.

Based on the velocity profiles taken at each location at different measurement planes, average mass flow rates were calculated using software package 'Surfer' by choosing a grid of 25 × 25 for each plane of measurement. The continuity of the flow both at the inlet and the outlet was checked for each case and was found to match within ± 1.5 per cent. Table 3 gives the percentage flow-split at dilution and primary holes in the outer and inner liner surfaces and swirlers. It is seen that approx. 42 to 45 per cent of the flow enters the liner through the outer dilution holes. Another 3 to 5 per cent of the flow goes through the outer primary holes. These flow-splits are in good agreement with the results predicted[14].

From Table 3, it is also seen that flow-split amongst the swirler, inner primary and dilution holes is affected by the inlet velocity. At the lower inlet velocity ($Re = 0.95 \times 10^4$), a large amount of the flow (33 per cent) goes through the cooling holes in the liner dome and the swirlers, while only 9.2 per cent and 13 per cent goes through the inner primary and dilution holes, respectively. At higher inlet velocity ($Re = 1.42 \times 10^4$), share for the swirlers and the liner dome cooling holes reduces to about 18.3 per cent and the flow-split through the inner primary and dilution holes increases to 8 per cent and 24 per cent, respectively. This change in the flow-split through the swirlers and inner dilution holes can be explained on the basis of velocity profiles which are uniformly distributed in the inner annular passage for the higher inlet velocity.

5. CONCLUSIONS

The following conclusions can be drawn based on the present study:

- Velocity measurement in the annuli of the plane reverse-flow model combustor shows flow to be nearly axial at each plane of measurement in the outer annular passage.

Table 3. Flow-split through different holes of the outer and the inner liner surfaces

Mean inlet velocity (m/s)	Liner surface	Type of holes	Percentage flow-split of inlet flow
11.8	Outer surface	Dilution	42.1
		Primary	3.0
	Liner dome	Cooling holes & swirlers	32.7
	Inner surface	Dilution	13.0
		Primary	9.2
17.7	Outer surface	Dilution	44.8
		Primary	4.6
	Liner dome	Cooling holes & swirlers	18.3
	Inner surface	Dilution	24.2
		Primary	8.1

- Due to the geometrical design of the combustor, the flow-splits through the outer and inner annular passages are different. About 45 to 49 per cent of the flow passes into the liner through the outer dilution and primary holes. The increase in the inlet velocity has no appreciable change in the flow pattern except for an increase of nearly 4 per cent in the total flow-split from outer annulus passage to the liner.

  The flow-split in the inner annular passage and the liner dome gets affected by the inlet velocity. At lower inlet velocity, significant portion of the flow passes through the swirlers and dome cooling holes (about 33 per cent), while for the higher inlet velocity, large portion of the flow goes through the inner dilution holes (about 24 per cent).

ACKNOWLEDGEMENTS

The authors acknowledge the support of Aeronautical Research & Development Board (ARDB) under the project ARDB-736 to carry out studies in reverse-flow combustors.

REFERENCES

Lefebvre, A. H. Gas turbine combustion, Ed. McGraw-Hill, New York, 1983.

2. Heitor, M.V. & Whitelaw, J.H. Velocity, temperature and species characteristics of the flow in a gas turbine combustor. *Combustion and Flame*, 1986, **64**, 1-32.

3. Bicen, A.F. & Jones, W.P. Velocity characteristics of isothermal and combusting flows. *Combust. Sci. Tech.*, 1986, **49**, 1-15.

4 Koutmos, P. & McGuirk, J. J. Investigation of swirler/dilution jet flow split on primary zone flow pattern in a water model can-type combustor. *J. Engg. Gas Turbine Power*, 1989, **111**, 310-17.

5 Cameron, C. D.; Brouwer, J. & Samuelsen, G. S. A model gas turbine combustor with wall jets and optical access for turbulent mixing, fuel effects and spray studies. Proceedings of the 22nd International Symposium on Combustion, 1988. pp. 465-74.

6. Bicen, A. F.; McGuirk, J. J. & Plama, J. M. L. M. Modelling gas turbine combustor flow fields in isothermal flow experiments. Proceedings of the Institute of Mechanical Engineers, Part A. *J. Power Engg.*, 1989, **203**, 113-22.

McGuirk, J. J. & Palma, J. M. L. M. Experimental investigation of the flow inside a water model of a gas turbine combustor; Part 1: Mean and turbulent flow field. *J. Fluids Engg.*, 1995, **117**, 450-58.

8. Bicen, A. F.; Tse, D. & Whitelaw, J. H. Flow and combustion characteristics of an annular combustor. *Combustion and Flame*, 1988, **72**, 175-92.

9. Cadiou, A. & Grienche, G. Experimental study of a reverse-flow combustor: Influence of primary holes on combustion efficiency. Paper presented at the Gas Turbine and Aeroengine Congress and Exposition, 4-8 June 1989, Toronto, Canada. Paper No. ASME-89-GT-249. pp 1-7.

10. Hu, T. C. J.; Cusworth, R. A. & Sislian, J. P. An experimental and computational investigation of an annular reverse-flow combustor. Institute for Aerospace Studies, University of Toronto, 1990. 135 p. Report No. UTIAS-338.

Siu, Y.W. Velocity measurements in models of a reverse-flow combustor. Imperial College of Science, Technology and Medicine, London, 1991. pp. 46-56. MS Thesis.

12. Riddlebaugh, S. M.; Lipshitz, A. & Greber, I. Dilution jet behaviour in the turn section of a reverse-flow combustor. AIAA Paper No. 82-0192, 1982. pp. 1-13; NASA-TM-82776.

13 Joos, F. & Simon, B. Comparison of the performance of the reverse-flow annular combustion chamber under low and high pressure conditions: Combustion and fuel in gas turbine engines. Advisory Group for Aerospace Research & Development, France, October 1987. Report No. AGARD-CP-422.

4. Bruce, T.W.; Mongia, H.C. & Reynolds, R. C. Combustor design criteria validation October 1978. Report No. US-ARTL-TR-78, .

5 Bharani, S.; Singh, S.N. & Agrawal, D.P. Velocity distribution in the buter annulus of a 120 sector model of a reverse-flow combustor. Proceedings of the 3rd National Conference on Air Breathing Engines and Aerospace Propulsion, 28-30 December 1996, Madras. pp. 135-44.

16. Mohan, R.; Singh, S. N. & Agrawal, D.P. Flow splits in a reverse-flow combustor. Proceedings of the 22nd National Conference on Fluid Mechanics and Fluid Power, 13-15 December 1995, Madras. India. pp. 182-86.